Electronic Structures and Thermochemical Properties of the Small Silicon-Doped Boron Clusters BnSi (n=1–7) and Their Anions

ARTICLE *in* CHEMPHYSCHEM · NOVEMBER 2011

Impact Factor: 3.42 · DOI: 10.1002/cphc.201100341 · Source: PubMed

6 AUTHORS, INCLUDING:

Truong Tai
University of Leuven
65 PUBLICATIONS **506** CITATIONS
SEE PROFILE

Devashis Majumdar
Jackson State University
90 PUBLICATIONS **1,558** CITATIONS
SEE PROFILE

Minh Tho Nguyen
University of Leuven
748 PUBLICATIONS **10,835** CITATIONS
SEE PROFILE

CHEMPHYSCHEM

DOI: 10.1002/cphc.201100341

Electronic Structures and Thermochemical Properties of the Small Silicon-Doped Boron Clusters B_nSi ($n = 1–7$) and Their Anions

Truong Ba Tai,[a] Paweł Kadłubański,[b] Szczepan Roszak,[b] Devashis Majumdar,[c] Jerzy Leszczynski,[c] and Minh Tho Nguyen*[a, d]

We perform a systematic investigation on small silicon-doped boron clusters B_nSi ($n = 1–7$) in both neutral and anionic states using density functional (DFT) and coupled-cluster (CCSD(T)) theories. The global minima of these $B_nSi^{0/-}$ clusters are characterized together with their growth mechanisms. The planar structures are dominant for small B_nSi clusters with $n \leq 5$. The B_6Si molecule represents a geometrical transition with a quasi-planar geometry, and the first 3D global minimum is found for the B_7Si cluster. The small neutral B_nSi clusters can be formed by substituting the single boron atom of B_{n+1} by silicon. The Si atom prefers the external position of the skeleton and tends to form bonds with its two neighboring B atoms. The larger B_7Si cluster is constructed by doping Si-atoms on the symmetry axis of the B_n host, which leads to the bonding of the silicon to the ring boron atoms through a number of hyper-coordination. Calculations of the thermochemical properties of $B_nSi^{0/-}$ clusters, such as binding energies (BE), heats of formation at 0 K (ΔH_f^0) and 298 K ($\Delta H_f^{[298]}$), adiabatic (ADE) and vertical (VDE) detachment energies, and dissociation energies (D_e), are performed using the high accuracy G4 and complete basis-set extrapolation (CCSD(T)/CBS) approaches. The differences of heats of formation (at 0 K) between the G4 and CBS approaches for the B_nSi clusters vary in the range of 0.0–4.6 kcal mol^{-1}. The largest difference between two approaches for ADE values is 0.15 eV. Our theoretical predictions also indicate that the species B_2Si, B_4Si, B_3Si^- and B_7Si^- are systems with enhanced stability, exhibiting each a double (σ and π) aromaticity. B_5Si^- and B_6Si are doubly antiaromatic (σ and π) with lower stability.

1. Introduction

Binary clusters based on boron are intriguing systems, in part due to their interesting but unusual properties and potential applications. Extensive experimental and theoretical studies on mixed clusters containing boron and transition metals or main-group elements have been reported.[1–8] The chemical bonding, and in particular the aromaticity of a few mixed and small-size B_nM clusters (where M are alkali and alkaline-earth metals such as Li, Na, Mg and Be), have been investigated theoretically.[9–12] A systematic investigation on lithium-doped boron clusters ($B_nLi^{0/-}$, $n = 1–8$) in both neutral and anionic states was carried out by some of us using high-level theoretical methods.[13] Similar theoretical investigations on aluminum-doped boron clusters (B_nAl, $n = 1–12$) are also available.[14] On the other hand, extensive experimental and theoretical studies on carbon–boron mixed clusters have been carried out[15–17] since a prediction on the existence of planar hexa-coordinated carbon in B_6C^{2-} clusters.[15]

Boron–silicon compounds have attracted considerable interest due to their potentially important applications in the fields of semiconductor materials and thermoelectric devices. A study of phase diagrams of the boron–silicon binary systems indicated the existence of two kinds of B_nSi compounds in the boron-rich region ($n = 16–26$ and also B_6Si).[18] The $B_{14}Si$ cluster was synthesized for the first time by Giese et al.,[19] and Imai et al. presented X-ray images and studies of the electronic properties of singlet crystal $B_{18}Si$.[20] However, in spite of the demonstrated importance of the boron–silicon compounds, the understanding of the electronic and thermodynamic properties of these materials is still very limited. To the best of our knowledge, only a few studies on small B_nSi clusters have been carried out. A theoretical study on the structure of the cationic clusters B_nSi^+ ($n = 1–4$) [21] and the BSi dimer was reported earlier.[22] BSi was first detected in mass spectrometry experiment, and other experimental and theoretical results on this molecule are also available.[23–25] More recently, predictions of the

[a] T. B. Tai, Prof. M. T. Nguyen
Department of Chemistry
Katholieke Universiteit Leuven
B-3001 Leuven (Belgium)
E-mail: minh.nguyen@chem.kuleuven.be

[b] P. Kadłubański, Prof. S. Roszak
Institute of Physical and Theoretical Chemistry
Wroclaw University of Technology
Wybrzeze Wyspianskiego 27, 50-370 Wroclaw (Poland)

[c] Prof. D. Majumdar, Prof. J. Leszczynski
Interdisciplinary Center for Nanotoxiciy
Department of Chemistry, Jackson State University
Jackson, MS 39217 (USA)

[d] Prof. M. T. Nguyen
Institute for Computational Science and
Technology of HoChiMinh City, Thu Duc
HoChiMinh City (Vietnam)

Supporting information for this article is available on the WWW under http://dx.doi.org/10.1002/cphc.201100341.

structure, energies and vibrational spectra of the triatomic B_2Si were obtained using the HF, B3LYP, CCSD(T) and CASSCF calculations.[26]

In view of the scarcity of reliable information on these binary systems, we set out to carry out a theoretical investigation on the silicon doped boron clusters B_nSi with n up to 7, where the first three-dimensional global minimum is located. This is of interest as the first 3D structure of pure boron clusters was found at a much larger size of $n=20$. In addition, the anionic clusters B_nSi^- that are relevant subjects for experimental photoelectron spectroscopic studies are also considered. Thermochemical properties such as binding energies, heats of formation, adiabatic and vertical detachment energies and dissociation energies of the clusters considered are evaluated using the composite G4 model, and the coupled-cluster theory CCSD(T) at the complete basis-set limit (CBS). Where available, experimental data are used for the calibration of computed results. The chemical bonding and aromaticity of the closed-shell systems are also analyzed using the canonical molecular orbitals (CMOs).

2. Computational Methods

Electronic structure calculations were carried out using the Gaussian 03[27] and Molpro 2008[28] program packages. Initial structures of the B_nSi clusters were manually constructed by either substituting a single boron atom of the pure B_{n+1} clusters reported previously by one silicon atom, or doping the silicon atom into pure B_n at various positions. Due to the small size of the clusters considered, the total number of isomers for each size was rather limited. Thus, we trust that all possible initial structures were included in our search for the global minima. Equilibrium geometries and vibrational frequencies of these initial structures B_nSi and their anions were determined using the hybrid B3LYP functional[29–31] in conjunction with the split-valence polarized 6-311+G(d) basis set of atoms.[32–34]

Enthalpies of formation for the global minima were evaluated from the corresponding total atomization energies (TAE).[35] Two sets of calculations were performed, including the coupled-cluster theory whose total energies were extrapolated to the complete basis-set limit, CCSD(T)/CBS, as previously used for the series of small boron clusters,[36,37] and the composite G4 approach.[38]

In the CCSD(T)/CBS approach, geometrical parameters were fully optimized using either the coupled-cluster CCSD(T) theory[39] (for small species $B_nSi^{0/-}$ with $n=1$–3), or the second-order perturbation theory (MP2) levels (for the larger species with $n=4$–7) using the correlation consistent aug-cc-pVTZ basis set. The unrestricted formalism (UHF, UMP2, UCCSD) was used for computing the total energies of the open-shell systems in the geometry optimizations. The total electronic energies were subsequently computed using the CCSD(T)[40] theory and then extrapolated to the complete basis set (CBS) limit. Single-point electronic energies were subsequently calculated using the restricted/unrestricted coupled-cluster (R/UCCSD(T)) formalism[41–43] with the aug-cc-pVnZ ($n=$D, T, and Q) basis sets on the (U)CCSD(T)/aug-cc-pVTZ and (U)MP2/aug-cc-pVTZ-optimized geometries. For simplicity, the basis sets were labeled as aVnZ. The CCSD(T) energies were extrapolated to the CBS limit energies using the expression (1):[44]

$$E(x) = A_{CBS} + B\exp[-(x-1)] + C\exp[-(x-1)^2] \quad (1)$$

where $x=2$, 3, and 4 for the aVnZ basis with $n=$D, T, and Q, respectively. Total CCSD(T) electronic energies as a function of basis set are given in Table S1 of the Supporting Information). Additional smaller corrections were also included in the TAE evaluations. Core–valence corrections (ΔE_{CV}) were obtained at the CCSD(T)/aug-cc-pwCVTZ level of theory.[45] Douglas–Kroll–Hess (DKH) scalar relativistic corrections ($\Delta E_{DKH\text{-}SR}$), which account for changes due to relativistic contributions to total energies of the molecule and constituent atoms, were calculated using the spin-free, one-electron DKH Hamiltonian.[46–48] $\Delta E_{DKH\text{-}SR}$ is defined as the difference in the atomization energy between the results obtained from basis sets re-contracted for DKH calculations,[49] and the atomization energy obtained with the normal valence basis set of the same quality. The DKH calculations are obtained as the differences of the results from the CCSD(T)/cc-pVTZ and the CCSD(T)/cc-pVTZ-DK levels of theory. Finally, spin–orbit (SO) corrections of 0.03 kcal mol^{-1} for the B atom, and 0.43 kcal mol^{-1} for the Si atom were obtained from the excitation energies of Moore.[50] The total atomization energy (ΣD_0 or TAE) of a compound is given by Equation (2):

$$\Sigma D_0 = \Delta E_{elec}(CBS) + \Delta E_{CV} + \Delta E_{DKH\text{-}SR} + \Delta E_{SO} - \Delta E_{ZPE} \quad (2)$$

By combining our computed ΣD_0 values, determined from either the CBS or the G4 calculations, with the known experimental heats of formation at 0 K for the elements B and Si, we can derive ΔH_f° values at 0 K for the molecules in the gas phase. Herein, we use the values $\Delta H_f^\circ(B) = 135.1 \pm 0.2$ kcal mol^{-1}, and $\Delta H_f^\circ(Si) = 107.2 \pm 0.2$ kcal mol^{-1}.[51] The rationale for this selection was discussed in our previous work.[36,37] We thus obtained heats of formation at 298 K by following the classical thermochemical procedure.[52] The calculated heats of formation at 0 K were used to evaluate the adiabatic detachment energy and other energetic quantities.[49] The natural bond orbitals (NBO)[53] were constructed using the B3LYP/6-311+G(d) densities.

3. Results and Discussion

The shapes of the equilibrium structures of the B_nSi and B_nSi^- clusters and their relative energies and symmetry point groups are shown in Figures 1 and 2. The different components obtained in the CBS protocol for total atomization energies (ΣD_0) of B_nSi and B_nSi^- are given in Table 1, and the total G4 and CBS energies are summarized in Table S1 of the Supporting Information. The heats of formation of the clusters derived using the ΣD_0 values obtained from both CBS and G4 methods are given in Table 2. The binding energies (BE) are tabulated in Table 3. The adiabatic (ADE) and vertical (VDE) detachment energies of B_nSi^- anions computed using both G4 and CBS methods are given in Table 4.

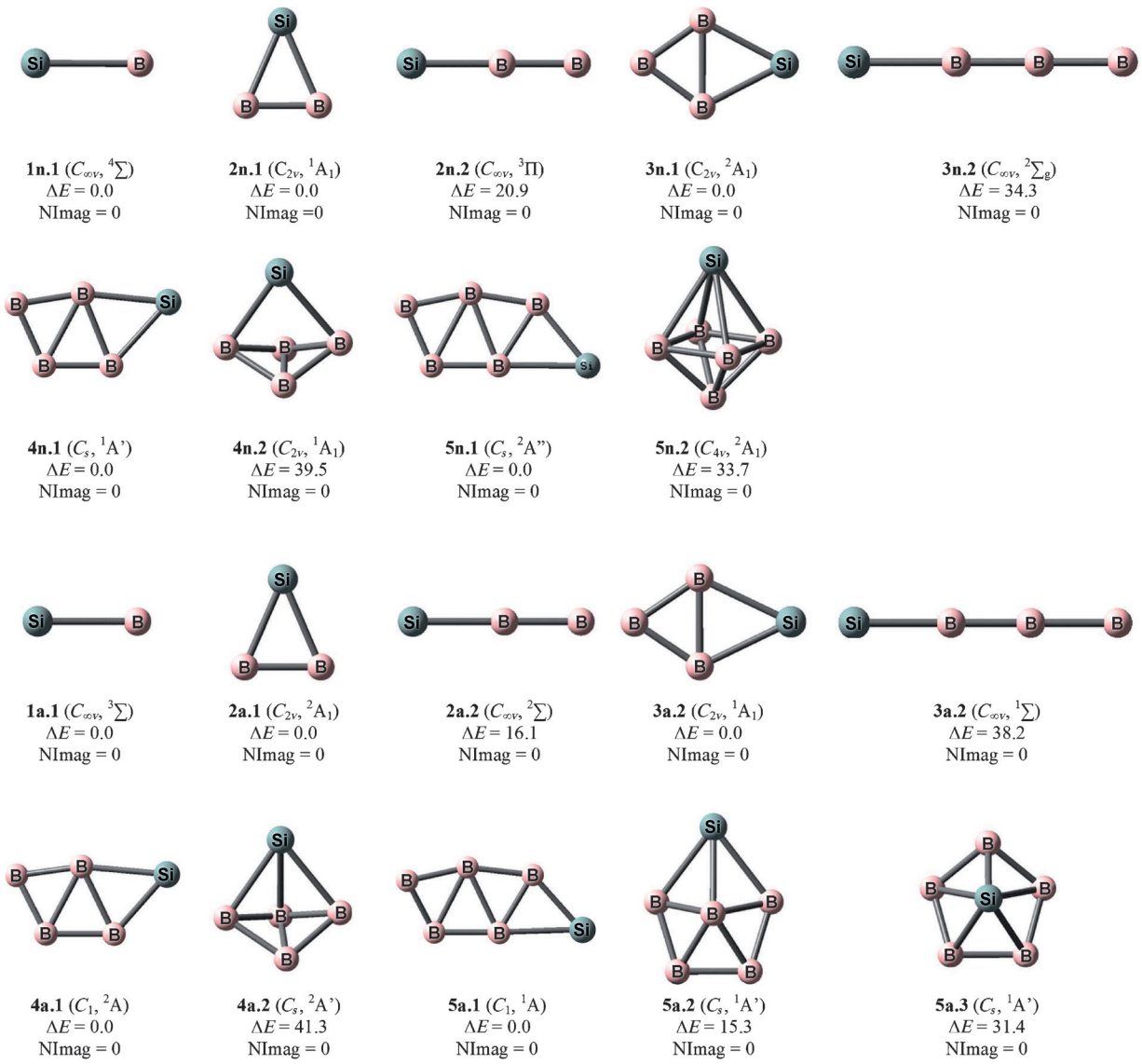

Figure 1. Structures, relative energies (kcal mol^{-1}), number of imaginary frequencies and point groups of the low-lying structures of B_nSi and B_nSi^- (n = 1–5) using the B3LYP/6-311 + G(d) level.

At a first glance, there is a good agreement between both sets of CBS and G4 results. The heats of formation at 0 K (ΔH^0_f) obtained by the CBS method (and listed in Table 2) are somewhat larger than those obtained applying the composite G4 approach. The difference varies in the range of 0.0–4.6 kcal mol^{-1}. The adiabatic detachment energies (ADE) obtained from energy differences between the neutrals and their corresponding anions (Table 4) also reveal a good agreement between both theoretical approaches. The maximum difference of both sets of ADE values is 0.14 eV. These differences of energetic properties between both G4 and CBS approaches can be understood from the ways of computing single-point electronic energies, as well as the geometries of clusters used. While geometries of clusters are obtained at the CCSD(T)/aug-cc-pVTZ level (or MP2/aug-cc-pVTZ level for $B_nSi^{0/-}$ with n = 5–7) for the CBS/CCSD(T) method, the G4 approach uses the geometries obtained at a lower level of theory, B3LYP/6-31G(2*df*,*p*). Our calculations shown in Figure S5 of the Supporting Information reveal that the G4 bond distances are systemically shorter than those obtained at the MP2 or CCSD(T) levels. The latter methods produce accurate distances with respect to experiment.[25] The heats of formation of BSi at 298 K ($\Delta H_f^{[298]}$), obtained from CBS and G4 methods, amount to 169.2 and 168.1 kcal mol^{-1}, respectively. These theoretical values are comparable to the experimental value of 166.71 ± 3.34 kcal mol^{-1}[25] that was determined by using Knudsen cell mass spectrometry and the thermal functions based on a calculated frequency of 772 cm^{-1} for BSi. More importantly, due to the lack of available experimental data, this agreement lends us a confidence in thermal functions calculated for other clusters and allows an estimate on the accuracy of the calculated results.

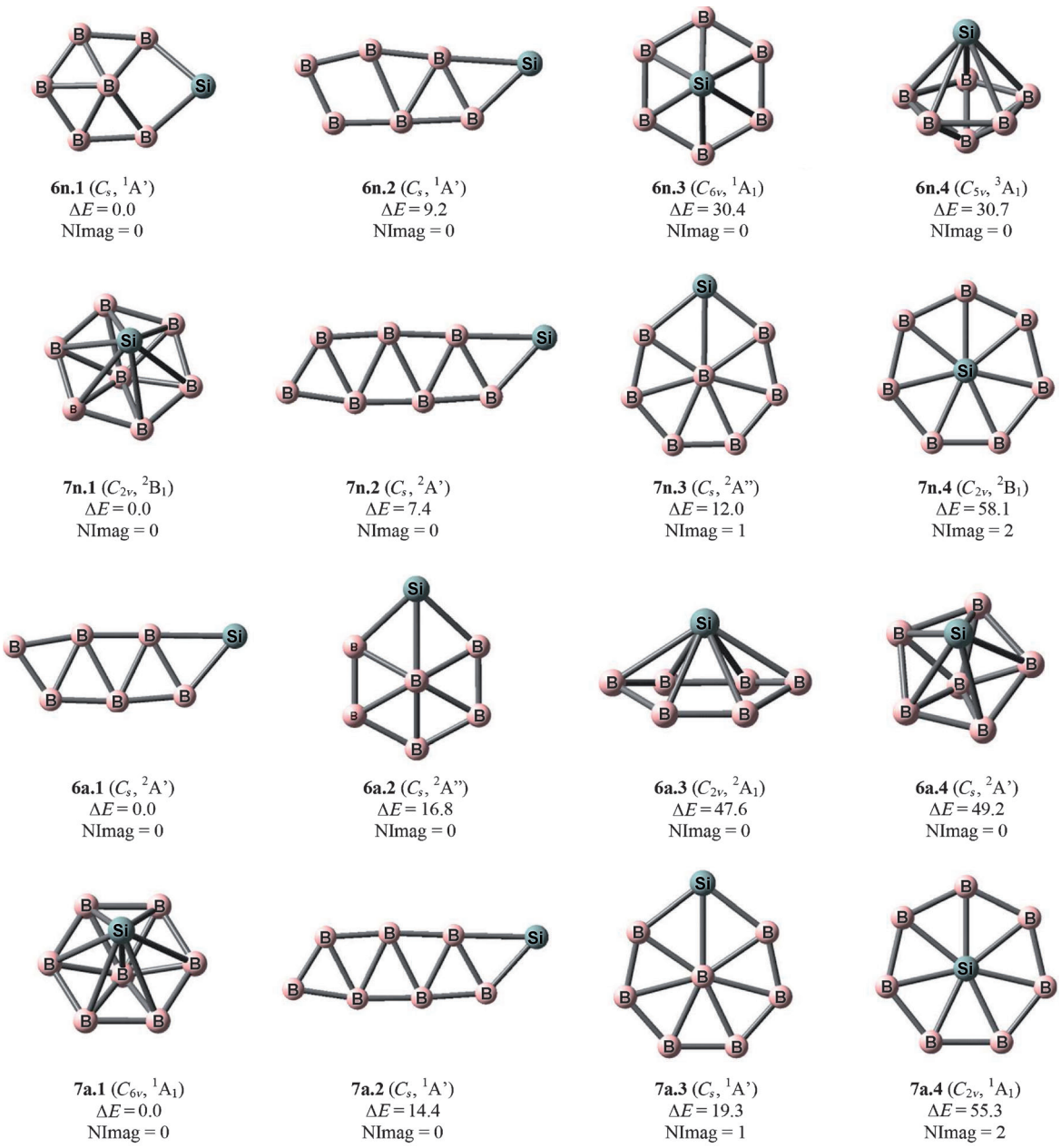

Figure 2. Geometries, relative energies (kcal mol^{-1}), number of imaginary frequencies and point groups of the low-lying structures of B_nSi and B_nSi^- (n = 6–7) using the B3LYP/6-311 + G(d) level.

Geometries of Lower-lying Isomers

In the following sections, the structures mentioned hereafter are labeled as ***n*n.x** and ***n*a.x**, in which ***n*** stands for the size, **n** a neutral form, and **a** an anion, and **x** denotes the ordering of isomer starting from the ***n*n.1** ground state.

BSi and BSi$^-$

The electronic ground state of BSi is characterized by the high spin $^4\Sigma^-$ with the [$^1\sigma^2 2\sigma^2 1\pi^2 3\sigma^1$] orbital configuration. This is in agreement with previous literature.[22,24] Similar to the diatomic B_2, the 1π bonding orbitals are lower in energy as compared to the 3σ bonding orbital. The doublet electronic state ($^2\Pi$) is significantly higher with a doublet–quartet separation of 31.4 kcal mol^{-1} (B3LYP/6-311 + G(d)). The bond length of the BSi ground state ($^4\Sigma^-$) amounts to 1.919 and 1.927 Å at the B3LYP/6-311 + G(d) and CCSD(T)/aug-cc-pVTZ levels, respectively.

Following attachment of one excess electron into π-bonding orbital, the high spin $^3\Pi$ state with the [$1\sigma^2 2\sigma^2 1\pi^2 2\pi^1 3\sigma^1$] orbital configuration becomes the ground state of BSi$^-$, with a singlet–triplet gap of 26.3 kcal mol^{-1}. The other high spin state ($^3\Sigma^+$) in which the 3σ bonding orbital is doubly occupied [$1\sigma^2 2\sigma^2 3\sigma^2 2\pi^2$] is 9.4 kcal mol^{-1} (0.41 eV) higher in energy with respect to the $^3\Pi$ ground state and could be considered as a low-lying excited state. The bond length of the anion BSi$^-$ ($^3\Pi$)

Table 1. CCSD(T)/CBS total atomic energy (TAE) [kcal mol^{-1}] for the neutral B_nSi and anionic B_nSi^- silicon-doped boron clusters ($n=1$–7) and the different components.

Molecule	ΔCBS[a]	ΔE_{ZPE}[b]	ΔE_{CV}[c]	ΔE_{SR}[d]	ΔE_{SO}[e]	TAE (0 K)
BSi^- ($C_{\infty v}$, $^3\Pi$)	113.84	1.12	0.60	−0.27	−0.46	112.58
BSi ($C_{\infty v}$, $^4\Sigma^-$)	75.17	1.05	0.63	−0.11	−0.46	74.18
B_2Si^- (C_{2v}, $^2A_1$)	241.79	3.88	1.98	−0.39	−0.49	239.01
B_2Si (C_{2v}, $^1A_1$)	195.70	3.49	1.85	−0.31	−0.49	193.27
B_3Si^- (C_{2v}, $^1A_1$)	363.37	6.24	3.43	−0.50	−0.52	359.53
B_3Si (C_{2v}, $^2A_1$)	301.03	5.85	3.21	−0.37	−0.52	297.50
B_4Si^- (C_1, ^2A)	473.15	9.08	4.58	−0.55	−0.55	467.56
B_4Si (C_s, $^1A'$)	428.76	8.68	4.44	−0.42	−0.55	423.55
B_5Si^- (C_s, $^1A'$)	595.84	11.82	5.99	−0.64	−0.58	588.78
B_5Si (C_s, $^2A''$)	531.05	12.29	5.76	−0.49	−0.58	523.45
B_6Si^- (C_s, $^2A'$)	724.60	15.08	7.66	−0.71	−0.61	715.86
B_6Si (C_s, $^1A'$)	661.92	14.55	7.33	−0.67	−0.61	653.41
B_7Si^- (C_{6v}, $^1A_1$)	879.49	17.79	9.55	−0.80	−0.64	869.81
B_7Si (C_{2v}, $^2B_1$)	796.50	18.42	9.57	−0.66	−0.64	786.36

[a] Extrapolated by using Equation (1) with the aVDZ, aVTZ and aVQZ basis sets. [b] Zero-point energies taken from the CCSD(T) harmonic frequencies for small clusters $B_nSi^{0/-}$ ($n=1$–3) and the MP2 harmonic frequencies for larger clusters $B_nSi^{0/-}$ ($n=4$–7). [c] Core–valence corrections obtained with the aug-cc-pwCVTZ basis sets at the optimized CCSD(T) or MP2 geometries. [d] Scalar relativistic correction based on a CCSD(T)-DK/cc-pVTZ-DK calculation and is expressed relative to the CCSD(T) result without the DK correction. [e] Correction due to the incorrect treatment of the atomic asymptotes as an average of spin multiplets. Values based on C. Moore's Tables, ref. [50].

Table 2. Heats of formation at 0 K (ΔH_f^0) and 298 K (ΔH_f^{298}) [kcal mol^{-1}] of neutral B_nSi and anionic B_nSi^- clusters ($n=1$–7) using CCSD(T)/CBS and G4 approaches.

Molecule	ΔH [0 K]		ΔH [298 K]	
	CBS	G4	CBS	G4
BSi^- ($C_{\infty v}$, $^3\Pi$)	129.7	128.1	130.8	129.2
BSi ($C_{\infty v}$, $^4\Sigma^-$)	168.1	167.1	169.2	168.1
B_2Si^- (C_{2v}, $^2A_1$)	138.4	133.8	139.6	135.5
B_2Si (C_{2v}, $^1A_1$)	184.1	180.6	185.3	181.8
B_3Si^- (C_{2v}, $^1A_1$)	153.0	150.9	154.4	152.3
B_3Si (C_{2v}, $^2A_1$)	215.0	215.3	216.5	216.8
B_4Si^- (C_1, ^2A)	180.0	175.8	181.7	177.4
B_4Si (C_s, $^1A'$)	224.1	223.3	225.7	225.0
B_5Si^- (C_s, $^1A'$)	193.9	191.5	195.6	193.3
B_5Si (C_s, $^2A''$)	259.3	257.4	260.9	259.5
B_6Si^- (C_s, $^2A'$)	201.9	198.7	203.8	200.5
B_6Si (C_s, $^1A'$)	264.4	264.4	266.0	266.0
B_7Si^- (C_{6v}, $^1A_1$)	183.1	181.7	184.6	183.1
B_7Si (C_{2v}, $^2B_1$)	266.5	265.2	268.0	266.7

Table 3. Average binding energy (BE, eV) and HOMO–LUMO gaps (HLG, eV) of neutral B_nSi and anionic B_nSi^- clusters ($n=1$–7).[a]

Isomers	BE		HLG	Isomers	BE		HLG
	G4	CBS			G4	CBS	
BSi ($C_{\infty v}$, $^4\Sigma^-$)	1.63	1.61	–	BSi^- ($C_{\infty v}$, $^3\Pi$)	1.80	1.74	–
B_2Si (C_{2v}, $^1A_1$)	2.84	2.79	2.48	B_2Si^- (C_{2v}, $^2A_1$)	3.07	2.99	–
B_3Si (C_{2v}, $^2A_1$)	3.22	3.20	–	B_3Si^- (C_{2v}, $^1A_1$)	3.58	3.55	2.71
B_4Si (C_s, $^1A'$)	3.68	3.67	2.91	B_4Si^- (C_1, ^2A)	3.82	3.78	–
B_5Si (C_s, $^2A''$)	3.80	3.78	–	B_5Si^- (C_s, $^1A'$)	4.05	4.02	1.62
B_6Si (C_s, $^1A'$)	4.05	4.05	3.40	B_6Si^- (C_s, $^2A'$)	4.26	4.24	–
B_7Si (C_{2v}, $^2B_1$)	4.27	4.26	–	B_7Si^- (C_{6v}, $^1A_1$)	4.55	4.54	4.25

[a] BEs are obtained using CCSD(T)/CBS and G4 approaches, HOMO–LUMO obtained at the B3LYP/6-311+G(d) level.

of 1.886 Å (CCSD(T)/aug-cc-pVTZ) is shorter than that of the neutral BSi (1.927 Å). With respect to the present CCSD(T) data, previous MP2 calculations[25] slightly underestimated the B–Si bond length (1.905 Å) in the diatomic BSi species.

B_2Si and B_2Si^-

The most stable B_2Si isomer (B3LYP/6-311+G(d) level) has a C_{2v} shape **2n.1** in which the Si atom is bridged with two B atoms (Figure 1). While the linear **2n.2** is the next isomer with a relative energy of 20.9 kcal mol^{-1}, the BSiB form is a stationary point with two imaginary frequencies. These results agree with a previous report by Davy et al.[26] In the anionic state, **2a.1** (C_{2v}, $^2A_1$) is the lowest-lying isomer and is formed by addition of one excess electron into the neutral **2n.1**. The linear structure **2a.2** is again the next isomer with an energy separation of 16.1 kcal mol^{-1}. As indicated by electron-charge distribution, the molecule is formed with small charge transfer. The HOMO, which is carrying a large part of the Si lone electron pair, possesses a σ character. The structure is stabilized by π HOMO-1 possessing 3center-2electron characteristics. Addition of an electron does not change the MO picture and the excess electron goes to the σ LUMO localized on the B–B fragment.

B_nSi and B_nSi^- ($n=3$–5)

Structures of B_nSi with $n=3$–5 are constructed by either substituting one B of the B_{n+1} isomers at various positions by the single Si atom, or connecting the silicon with the B_n isomers. While a full picture of all isomers located is given in Figure S1 of the Supporting Information, some isomers with low relative energies are displayed in Figure 1. It is interesting to note that the geometries of the global minima of B_nSi are similar to those of B_{n+1}. The **3n.1** (C_{2v}, $^2A_1$), **4n.1** (C_s, $^1A'$) and **5n.1** (C_s, $^2A'$) are the global minima of the B_3Si, B_4Si and B_5Si, respectively. Following attachment of an excess electron, the geometries of the corresponding anions (B_nSi^-) retain the structures their neutral counterparts with slight distortions. Consequently, **3a.1** (C_{2v}, $^1A_1$), **4a.1** (C_1, ^2A) and **5a.1**

Table 4. Adiabatic (ADE) and vertical (VDE) detachment energies [eV] of the anionic B_nSi^- clusters ($n=1-7$) using both CCSD(T)/CBS and G4 approaches.

Anions	Neutrals	ADE		VDE	
		CBS	G4	Neutral state	CBS
1a.1 ($C_{\infty v}$, $^3\Pi$)	1n.1 ($C_{\infty v}$, $^4\Sigma^-$)	1.67	1.69	BSi ($C_{\infty v}$, $^4\Sigma^-$)	1.72
2a.1 (C_{2v}, $^2A_1$)	2n.1 (C_{2v}, $^1A_1$)	1.99	2.03	B_2Si (C_{2v}, $^1A_1$)	2.00
3a.1 (C_{2v}, $^1A_1$)	3n.1 (C_{2v}, $^2A_1$)	2.79	2.79	B_3Si (C_{2v}, $^2A_1$)	2.81
4a.1 (C_1, ^2A)	4n.1 (C_s, $^1A'$)	1.91	2.06	B_4Si (C_1, ^1A)	2.16
5a.1 (C_s, $^1A'$)	5n.1 (C_s, $^2A''$)	2.83	2.86	B_5Si (C_s, $^2A''$)	2.89
6a.1 (C_s, $^2A'$)	6n.1 (C_s, $^1A'$)	2.71	2.85	–	–
6a.1 (C_s, $^2A'$)	6n.2 (C_s, $^1A'$)	3.28	3.41	B_6Si (C_s, $^1A'$)	3.73
7a.1 (C_{6v}, $^1A_1$)	7n.1 (C_{2v}, $^2B_1$)	3.62	3.62	B_7Si (C_{6v}, $^2A_1$)	3.75

(C_s, $^2A'$) are also the global minima of the anionic clusters B_3Si^-, B_4Si^- and B_5Si^-, respectively. As shown in Figure 1, the other isomers are significantly less stable (at least 34 and15 kcal mol^{-1} higher for the neutral and anionic clusters, respectively). All of these ground-state isomers ($n=3$–5), in analogy to the pure boron complexes, are represented by "ribbon" topology of triangle B_3 building blocks. The Si atom is attached to the edge of the ribbon with two B–Si bonds. In the case of these clusters, the amount of electronic density donated from Si to the B_n fragment increases. This transfer is smaller in anions, although its value increases with the cluster size. The planar structures are stabilized by 3c–2e π orbital, but due to the size of molecules, its stability tends to decrease. The electron spin density indicates a preference for tail and head (Si atom) positions characterized by only two bonds (see Supporting Information). The general picture, however, is complicated by possible conjugations between boron atoms.

B_6Si and B_6Si^-

Various structures of the B_6Si are located including a C_s quasi-planar structure **6n.1** where one peripheral B of the hexagonal ring B_7 is actually replaced by Si. The others are a C_s structure (continuation of the ribbon sequence) **6n.2** in which Si substitutes single B of the zigzag B_7 form, and a C_{6v} structure **6n.3** in which Si is located on the C6 axis of the hexagonal ring (Figure 2). Although a planar isomer with peripheral Si (characterized by three B–Si bonds) is observed for smaller clusters (**4a.2, 5a.2**), it became ground state only in the B_6Si isomer. Our calculations show that **6n.1** is the global minimum of B_6Si. While **6n.2** is also a stable isomer (relative energy of 9.2 kcal mol^{-1}), the high symmetry **6n.3** isomer is much less stable. A high spin **6n.4** (C_{5v}, $^3A_1$) is also located, but it is higher in energy by 30.7 kcal mol^{-1}.

A reversed energetic ordering is observed for the B_6Si^- anions. The global minimum **6a.1** of B_6Si^- is formed by addition of an electron into **6n.2**. The **6a.2** isomer, which is formed from the minimum energy isomer of the neutral cluster **6n.1**, is now 16.8 kcal mol^{-1} higher in energy. Other forms are much less stable with relative energy of at least 47 kcal mol^{-1}. The charge distribution in "ribbon" isomers continues the trends observed for the smaller clusters. The density in "planar rings" is distributed differently with Si atom donating more electronic density to the boron ring.

B_7Si and B_7Si^-

The first 3D global minimum in the series of B_nSi is found for B_7Si. Unlike the B_nC clusters where the B_7C was reported to be a planar structure (C_s),[54] the global minimum of B_7Si is a 3D structure **7n.1** (C_{2v}, $^2B_1$) that is distorted from a high symmetry form (C_{6v}), with Si located on the C_6 axis of a bi-capped hexagonal ring. The planar "ribbon" structure **7n.2**, having a similar shape to the global minimum B_7C, is the second isomer with a relative energy of 7.4 kcal mol^{-1}. Other planar forms **7n.3** and **7n.4** rather represent transition states.

Following attachment of one excess electron, the high symmetry **7a.1** (C_{6v}) becomes the global minimum of B_7Si^-. **7a.2** (C_s) turns out to be the second isomer with relative energy of 7.4 kcal mol^{-1}. The B_6 base ring in bi-pyramids (both molecules and anions) is stabilized by electrons from off the base atoms. The ring also accommodates the excess electron in the case of this isomer. The 3D isomers are also found in smaller clusters (e.g. **6n3** isomer) but significantly higher in energy. The "benzene-like" hexagonal ring is observed as an element (building block) of boron nano-ribbons, but has to be stabilized by other atoms.

In general, planar "ribbon" structures are dominant for small clusters with $n \leq 5$. The B_6Si molecule can be considered as geometrical transition with a quasi-planar structure. The first 3D global minimum is found for the B_7Si. In the "ribbon-like" case, Si prefers a peripheral position of the ring and tends to bridge with its two B neighbors while its lone pair is located on the σ-type orbital. The unpaired boron electrons also occupy a σ molecular orbital allowing planar expansion of the clusters. B_7Si is constructed by doping Si on the symmetry axis of the B_n host where Si is bound to B atoms of the ring and possesses a high coordination number. The central B_6 ring is stabilized by electrons of plane atoms.

Energetic Properties

The relative stability of clusters is examined on the basis of the average binding energy (E_b) and the second-order difference in the total energies (Δ^2E) which are defined as follows [Eqs. (3)–(6)]:

$$E_b(B_nSi) = [nE(B) + E(Si) - E(B_nSi)]/(n+1) \quad (3)$$

$$E_b(B_nSi^-) = [nE(B) + E(Si^-) - E(B_nSi^-)]/(n+1) \quad (4)$$

$$\Delta^2E(B_nSi) = E(B_{n-1}Si) + E(B_{n+1}Si) - 2E(B_nSi) \quad (5)$$

$$\Delta^2E(B_nSi^-) = E(B_{n-1}Si^-) + E(B_{n+1}Si^-) - 2E(B_nSi^-) \quad (6)$$

While the average binding energies E_b of B_nSi in both neutral and anionic states are given in Table 3, the plots of these values and the second-order difference in energy (Δ^2E) are illustrated in Figures 3 and 4, respectively. To consider the effects of Si doping, binding-energy values of the B_n host are evaluated from total atomic energies (TAE) of the B_n clusters (obtained from refs. [36] and [37] at the same CBS method). Binding-energy values of B_n clusters are reported in Table S3 (Supporting Information), their plot is also shown in Figure 3. At a first glance, the average binding energies increase with the increasing boron number. While the B_nSi neutrals exhibit high BE values that can be comparable to those of pure B_n clusters, the BE values of B_nSi^- anions are slightly larger. This difference can be due to the BE values of the anionic boron clusters B_n^-, which are larger than those of the neutral B_n clusters.[8] Although the average binding energy is a suitable measure for the stability of clusters, there is no direct relation between the BE values of various charged systems.

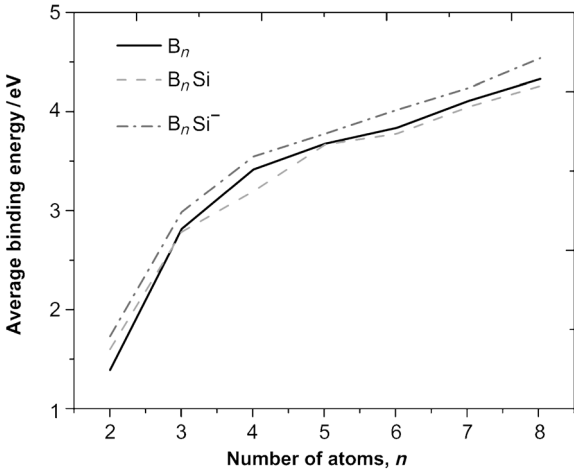

Figure 3. Average binding energy (BE) (eV) of the B_nSi clusters at the neutral and anionic states and the B_n clusters ($n=1$–7) using the CCSD(T)/CBS approach.

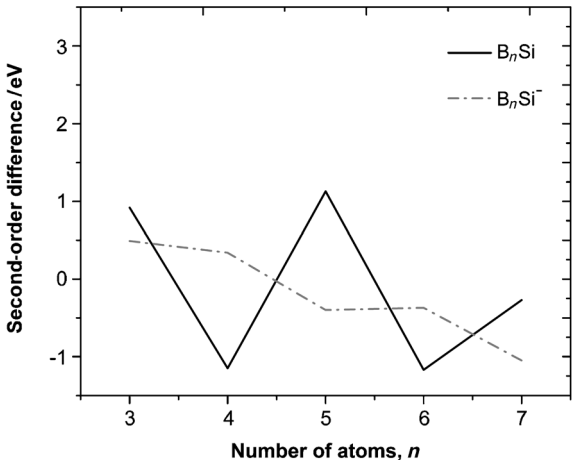

Figure 4. Second-order differences in energy (Δ^2E) of B_nSi clusters at both neutral and anionic states ($n=1$–7) using the CCSD(T)/CBS approach.

From the curves of the second-order difference (Δ^2E), the even–odd sequence is well visible and two local maximum peaks are found for B_nSi at sizes of $n=2$ and 4. In the case of anions, the Δ^2E values indicate B_2Si^- and B_3Si^- to be the more stable anions.

HOMO–LUMO Gaps

Frontier orbital energy gap (HLG) is considered as a measure of the kinetic stability of a molecule. A large gap indicates that the species possess high stability against chemical reactions. The HOMO–LUMO gaps of closed-shell $B_nSi^{0/-}$ are obtained using the B3LYP/6-311+G(d) level and are given in Table 3. B_7Si^- has a gap of 4.3 eV, being the largest value in the series of closed-shell species $B_nSi^{0/-}$.

Adiabatic (ADE) and Vertical (VDE) Detachment Energies

The electron-detachment energy can also be considered as a measure of the stability of an anion. A high ADE value indicates a stable anion with respect to electron ejection, whereas a low ADE suggests reluctance of the neutral counterpart to capture an electron. The ADE values of B_nSi^- obtained from the G4 and CBS calculations, listed in Table 4, show that there is a negligible difference between the values obtained from both methods. The largest difference amounts to 0.15 eV for B_4Si^-. Due to small geometrical distortions between the neutral species and the corresponding anions, the VDE values of the anions obtained from the CBS method are quite close to the ADE values. Two ADE values for B_6Si^- are obtained, including a value of 2.7 eV that is calculated from the energy difference between the two global minima **6a.1** and **6n.1**, and a value of 3.3 eV calculated from the global minimum **6a.1** and its corresponding neutral form **6n.2**. The later value of 3.3 eV is, as expected, closer to the VDE value of 3.7 eV.

Both ADE and VDE values of B_7Si^- are remarkably large as compared to smaller complexes. Additionally, the ADE and VDE values of B_2Si^- and B_4Si^- are considerably low. This indicates a high stability of the clusters B_7Si^-, B_2Si and B_4Si, which is consistent with the above predictions.

Dissociation Energies (D_e)

To probe further the thermodynamic stability of the clusters, we examine their dissociation energies. For the neutrals, the following reaction energies for the channels are considered [Eqs. (7) and (8)]:

$$B_nSi \rightarrow B_n + Si \quad (7)$$

and

$$B_nSi \rightarrow B_{n-1}Si + B \quad (8)$$

Table 5. Reaction enthalpies (ΔH^0, kcal mol^{-1}) of different dissociation channels.[a]

Neutrals	(7)	(8)	Anions	(9)	(10)	(11)	(12)
BSi ($C_{\infty v}$, $^4\Sigma^-$)	74.3	74.2	BSi^- ($C_{\infty v}$, $^3\Pi$)	80.8	106.8	106.8	80.7
B_2Si (C_{2v}, $^1A_1$)	129.0	119.1	B_2Si^- (C_{2v}, $^2A_1$)	142.8	129.7	159.0	126.4
B_3Si (C_{2v}, $^2A_1$)	102.3	104.2	B_3Si^- (C_{2v}, $^1A_1$)	132.4	97.9	160.5	120.5
B_4Si (C_s, $^1A'$)	107.8	126.1	B_4Si^- (C_1, ^2A)	119.9	113.0	164.3	108.0
B_5Si (C_s, $^2A''$)	99.7	99.9	B_5Si^- (C_s, $^1A'$)	133.1	112.2	159.4	121.2
B_6Si (C_s, $^1A'$)	130.0	130.0	B_6Si^- (C_s, $^2A'$)	160.6	124.9	186.6	127.1
B_7Si (C_{2v}, $^2B_1$)	122.8	133.0	B_7Si^- (C_{6v}, $^1A_1$)	174.3	145.8	210.6	154.0

[a] Values are evaluated from the CCSD(T)/CBS heats of formations at 0 K. The dissociation channels are: (**7**) $B_nSi \rightarrow B_n + Si$; (**8**) $B_nSi \rightarrow B_{n-1}Si + B$; (**9**) $B_nSi^- \rightarrow B_n + Si^-$ (**10**) $B_nSi^- \rightarrow B_n^- + Si$; (**11**) $B_nSi^- \rightarrow B_{n-1}Si + B^-$, and (**12**) $B_nSi^- \rightarrow B_{n-1}Si^- + B$

For the anionic clusters B_nSi^-, four dissociation channels [Eqs. (9)–(12)] are examined and the results are tabulated in Table 5:

$$B_nSi^- \rightarrow B_n + Si^- \quad (9)$$

$$B_nSi^- \rightarrow B_n^- + Si \quad (10)$$

$$B_nSi^- \rightarrow B_{n-1}Si + B^- \quad (11)$$

$$B_nSi^- \rightarrow B_{n-1}Si^- + B \quad (12)$$

The heats of formation of the boron clusters B_n of both the neutral and the anionic states used to calculate the dissociation energies (D_e) are taken from refs. [36] and [37]; these were obtained using the same CCSD(T)/CBS method. For the neutrals, the dissociation energies obtained from two channels are approximate, except for B_4Si. The D_e (107.8 kcal mol^{-1}) for the channel $B_4Si \rightarrow B_4 + Si$ is smaller as compared to that of 126.1 kcal mol^{-1} for the channel $B_4Si \rightarrow B_3Si + B$. This difference can be understood by the high stability of the fragment B_4. An even–odd oscillation is consistently observed in which the closed-shell systems show higher dissociation energies.

For anionic clusters, the dissociation energies (D_e) obtained from two channels: $B_nSi^- \rightarrow B_n + Si^-$ and $B_nSi^- \rightarrow B_{n-1}Si + B^-$ are similar and much higher in comparison to the other channels. For all the four channels considered, the D_e value of B_7Si is remarkably high, which again indicates its high thermodynamic stability.

Chemical Bonding and Aromaticity

The chemical bonding and aromaticity of the closed-shell species $B_nSi^{0/-}$ are probed using an analysis of CMO under the viewpoint of the Hückel rule of electron count.[55] Accordingly, the planar organic compounds possessing $(4N+2)$ delocalized valence electrons are considered to be aromatic, whereas the compounds with $4N$ delocalized valence electrons are anti-aromatic. This classical rule has been extensively applied for inorganic compounds as well as element clusters and more recently was successfully applied to evaluate the aromaticity of pure boron clusters B_n[8,15,36,56] and other clusters.[57]

The CMOs of B_2Si reveal that there is an analogy in MO pictures between the B_2Si (Figure 5a) and its isovalent to the B_3^- species.[56] While the HOMO of B_2Si is a delocalized σ-type MO, the HOMO-1 turns out to be a completely delocalized π-MO. Similar to B_3^-, the three remaining valence MOs, namely HOMO-2, HOMO-3 and HOMO-4, are σ orbitals to be localized into three two-center-two-electron (2c–2e) bonds and are responsible for localized bonds of B_2Si. Consequently, the B_2Si possesses two σ-type valence electrons and two π-type valence electrons that are globally delocalized over the system. According to the classical Hückel rule of $(4N+2)$ electrons, the neutral B_2Si is a doubly π and σ aromatic system that is consistent with its enhanced thermodynamic stability.

The closed-shell B_3Si^- is an interesting case, because its MO picture is similar to that of the well-known dianion B_4^{2-} (Figure 5b). The structural character and aromaticity of dianion B_4^{2-} are extensively studied using various methods.[56] It is shown to be a doubly (σ and π) aromatic system with a high resonance energy (RE). The MO picture of the B_3Si^- in Figure 5b reveals that its HOMO is a σ MO and is partially delocalized over the triangular B_3. HOMO-1 is a completely delocalized σ MO, and HOMO-2 is a completely delocalized π MO. The remaining orbitals, namely HOMO-3, HOMO-4, HOMO-5 and HOMO-6, are σ orbitals to be localized into four 2e–2c bonds and are thus responsible for localized bonds of B_3Si^-. As a consequence, B_3Si^- is expected to be a doubly (σ and π) aromatic system with two globally delocalized σ valence electrons and two π valence electrons that overall satisfy the Hückel rule.

Similar to B_3Si^-, the HOMO of B_4Si is a bonding σ MO, partially delocalized over the four-membered B_4 ring. While HOMO-1 is a completely delocalized σ MO, HOMO-3 is a π MO, which is globally delocalized over the entire system. The remaining MOs (HOMO-2, HOMO-4, HOMO-5, HOMO-6 and HOMO-7) are responsible for five 2e–2c bonds of the B_4Si. Consequently, B_4Si can be considered as a doubly (π and σ) aromatic system with two π electrons and two σ electrons that are globally delocalized.

A similar analysis is performed for the closed-shell species B_5Si^- and B_6Si. The HOMO and HOMO-4 of B_5Si^- are both globally delocalized π MOs that make B_5Si^- π anti-aromatic. While HOMO-2 and HOMO-3 are delocalized σ MOs, the remaining MOs are responsible for six 2c–2e bonds in this system. Having $2N$ electrons, B_5Si^- is doubly σ and π anti-aromatic with four globally delocalized σ valence electrons and four π valence electrons. Similarly, B_6Si is a doubly (π and σ) anti-aromatic system containing four delocalized σ-electrons (HOMO-1 and HOMO-2) and four delocalized π-electrons (HOMO and HOMO-6). These observations are consistent with the lower stability of both B_5Si^- and B_6Si.

The special stability of the three-dimensional structure B_7Si^- (C_{6v}) is of interest. The lower-lying orbitals, namely HOMO-3, HOMO-5, HOMO-5′, HOMO-7, HOMO-7′ and HOMO-8, are basi-

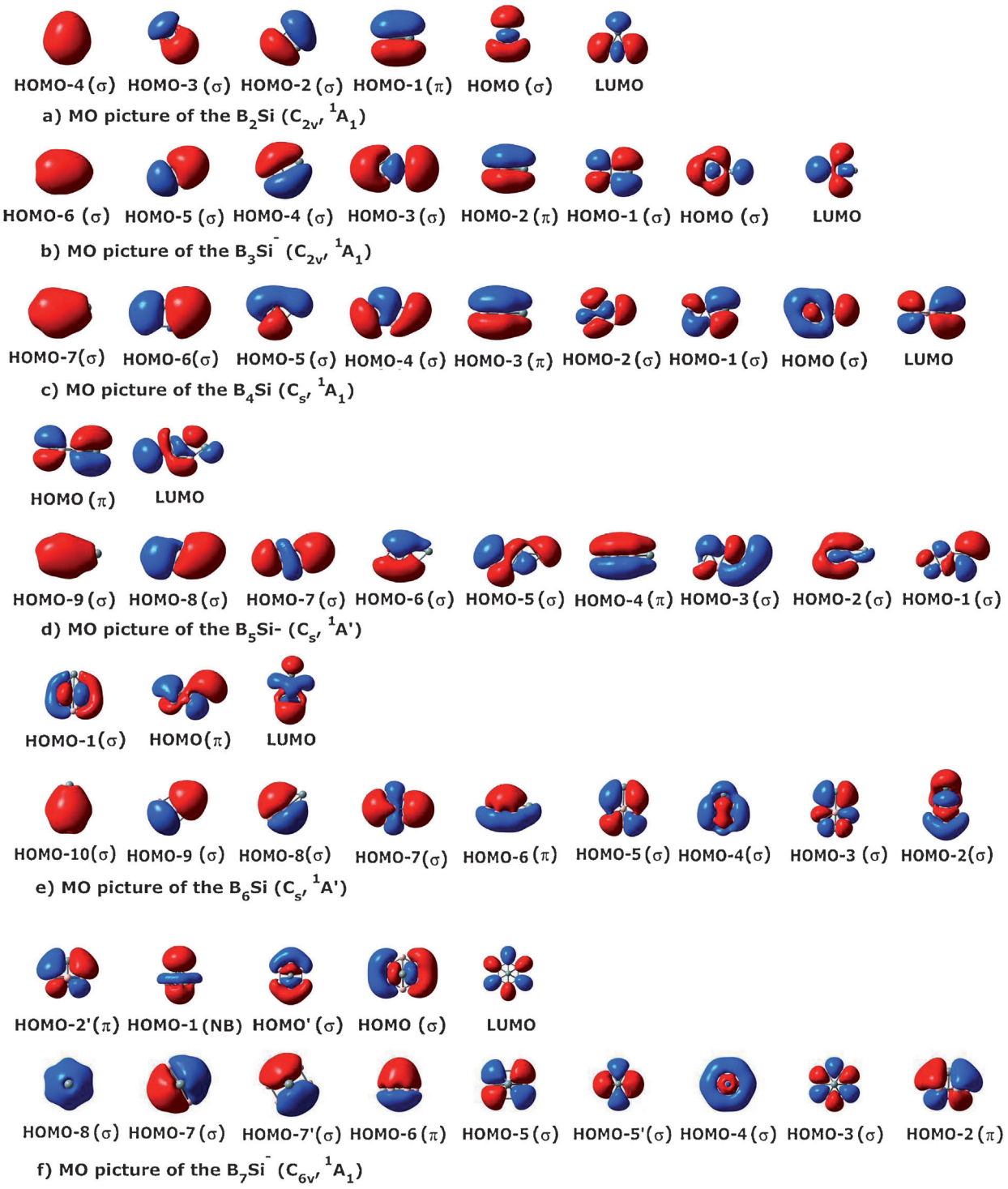

Figure 5. Shape of MOs of closed-shell systems considered using B3LYP/6-311 + G(d) densities.

cally localized into six peripheral B–B bonds of the hexagonal ring. The HOMO-1 is pointed out to be a non-bonding orbital. Consequently, the remaining MOs are globally delocalized and involved in the bonding of the hexagonal ring and between B and Si-atoms on the C_6 axis. The HOMO, HOMO′ and HOMO-4 are σ orbitals that are occupied by six delocalized σ electrons. The HOMO-2, HOMO-2′ and HOMO-6 are π orbitals and occupied by six delocalized π electrons. As a result, B_7Si^- behaves as a doubly (π and σ) aromatic system in the sense of the Hückel rule.

4. Conclusions

Herein, we perform a systematic investigation on small silicon-doped boron clusters B_nSi ($n = 1–7$) in both neutral and anionic states using the CCSD(T)/CBS and G4 methods. The global

minima $B_nSi^{0/-}$ are determined and the growth mechanism of the clusters emerges as follows:

i) Planar "ribbon" structures are dominant for small clusters B_nSi with $n \leq 5$. The B_6Si can be considered as a geometrical transition with quasi-planar structure, the first 3D global minimum is found for $n = 7$.

ii) B_nSi with $n \leq 6$ can be formed by substituting one B of the B_{n+1} with Si atom. Additionally, Si prefers a peripheral position of the ring and tends to connect with its two neighboring B atoms forming a bridge.

iii) B_7Si is built up by doping Si on the symmetry axis of the B_n host where Si is bound to B atoms of the ring and possesses a high coordination number.

The thermochemical properties of the $B_nSi^{0/-}$ clusters, such as binding energy (BE), heat of formation at 0 K (ΔH_f^0) and 298 K ($\Delta H_f^{[298]}$), adiabatic (ADE) and vertical detachment energy (VDE), and dissociation energy (D_e), are evaluated using the high-accuracy G4 and CCSD(T)/CBS methods. The calculated results obtained from both methods are compared to each other for the first time. The difference in calculated heats of formation for B_nSi varies in the range of 0.0–4.6 kcal mol^{-1}. The largest difference of 0.15 eV is found for the ADE values.

Our analysis of the MOs also demonstrates that the species B_2Si, B_4Si, B_3Si^- and B_7Si^- are systems with enhanced stability that exhibit a doubly (σ and π) aromatic character. Both B_5Si^- and B_6Si are doubly σ and π anti-aromatic systems. We hope that experimental studies on these interesting systems can be performed in a near future.

Supporting Information: The Supporting Information includes: the single-point electronic energies obtained at the CCSD(T)/auc-cc-pVnZ levels (n = D, T, Q) and their CBS values; the structures and relative energies of all the isomers, including the transition states; and the B3LYP-calculated Gibbs energy and heat content functions.

Acknowledgements

M.T.N. is indebted to the K.U. Leuven Research Council (GOA, IDO and IUAP programs) and thanks ICST for supporting his stays in Vietnam and JSU for his stays in Jackson, Mississippi. T.B.T. thanks the Arenberg Doctoral School for a scholarship.

Keywords: boron · clusters · computational chemistry · density functional theory · doping

[1] T. B. Tai, P. V. Nhut, M. T. Nguyen, S. Li, D. A. Dixon, *J. Phys. Chem. A* **2011**, *115*, 7673.
[2] Y. Qu, W. Ma, X. Bian, H. Tang, W. Tian, *Int. J. Quantum Chem.* **2006**, *106*, 960.
[3] S. Shahbazian, A. Sadjadi, *J. Mol. Struct. THEOCHEM.* **2007**, *822*, 116.
[4] C. Liu, M. Tang, H. Wang, *J. Phys. Chem. A* **2007**, *111*, 704.
[5] a) J. M. L. Martin, P. R. Taylor, *J. Chem. Phys.* **1994**, *100*, 9002; b) J. M. L. Martin, J. E. Yazal, J. O. Francois, *Chem. Phys. Lett.* **1996**, *248*, 95.
[6] H. J. Zhai, L. S. Wang, D. Y. Zubarev, A. I. Boldyrev, *J. Phys. Chem. A* **2006**, *110*, 1689.
[7] J. Saloni, P. Kadłubanski, S. Roszak, D. Majumdar, G. Hill, Jr., J. Leszczynski, *ChemPhysChem* **2011**, *12*, 1358.
[8] a) T. B. Tai, M. T. Nguyen, *Chem. Phys. Lett.* **2009**, *483*, 35; b) T. B. Tai, M. T. Nguyen, D. A. Dixon, *J. Phys. Chem. A* **2010**, *114*, 2893.
[9] a) Q. S. Li, Q. Jin, *J. Phys. Chem. A* **2004**, *108*, 855; b) Q. S. Li, Q. Jin, *J. Phys. Chem. A* **2003**, *107*, 7869.
[10] L. F. Gong, W. L. Guo, X. M. Wu, Q. S. Li, *Chem. Phys. Lett.* **2006**, *429*, 326.
[11] A. N. Alexandrova, A. I. Boldyrev, H. J. Zhai, L. S. Wang, *J. Chem. Phys.* **2005**, *122*, 054313.
[12] A. N. Alexandrova, H. J. Zhai, L. S. Wang, A. I. Boldyrev, *Inorg. Chem.* **2004**, *43*, 3552.
[13] a) T. B. Tai, M. T. Nguyen, *Chem. Phys.* **2010**, *375*, 35; b) M. T. Nguyen, *J. Mol. Struct. THEOCHEM* **1986**, *136*, 371; c) M. T. Nguyen, *Mol. Phys.* **1986**, *58*, 655.
[14] X. J. Feng, Y. H. Luo, *J. Phys. Chem. A* **2007**, *111*, 2420.
[15] L. M. Wang, B. B. Averkiev, J. A. Ramilowski, W. Huang, L. S. Wang, A. I. Boldyrev, *J. Am. Chem. Soc.* **2010**, *132*, 14104, and references therein.
[16] R. M. Minyaev, T. N. Gribanova, A. G. Starikov, V. I. Minkin, *Mendeleev Commun.* **2001**, *11*, 213.
[17] R. Islas, T. Heine, K. Ito, P. v. R. Schleyer, G. Merino, *J. Am. Chem. Soc.* **2007**, *129*, 14767.
[18] B. Armas, G. Male, D. Salanoubat, C. Chatillon, M. Allibert, *J. Less-Common Met.* **1981**, *82*, 245.
[19] R. F. Giese, J. Economy, V. I. Z. Matkovich, *Kristallografiya* **1965**, *122*, 144.
[20] M. Imai, T. Kimura, K. Sato, T. Hirano, *J. Alloys Compd.* **2000**, *306*, 197.
[21] D. N. Bernardo, G. H. Morrison, *Surf. Sci.* **1989**, *223*, L913.
[22] A. I. Boldyrev, J. Simons, *J. Phys. Chem.* **1993**, *97*, 1526.
[23] G. Verhaegen, F. E. Stafford, M. Ackerman, J. Drowart, *Nature* **1962**, *193*, 1280.
[24] L. B. Knight, Jr., A. J. McKinley, R. M. Babb, M. D. Morse, C. A. Arrington, *J. Chem. Phys.* **1993**, *98*, 6749.
[25] R. Viswanathan, R. W. Schmude, K. A. Gingerich, *J. Phys. Chem.* **1996**, *100*, 10784.
[26] R. Davy, E. Skoumbourdis, D. Dinsmore, *Mol. Phys.* **2005**, *103*, 611.
[27] Gaussian 03 (Revision C.01), M. J. Frisch, et al. Gaussian, Inc., Wallingford CT, **2004**.
[28] MOLPRO, version 2008.1, a package of *ab initio* programs, H.-J. Werner, et al.
[29] R. G. Parr, W. Yang, *Density-Functional Theory of Atoms and Molecules*, Oxford University Press, Oxford, **1989**.
[30] A. D. Becke, *J. Chem. Phys.* **1993**, *98*, 5648.
[31] J. P. Perdew, J. A. Chevary, S. H. Vosko, K. A. Jackson, M. R. Pederson, D. J. Singh, C. Fiolhais, *Phys. Rev. B* **1992**, *46*, 6671.
[32] T. Clark, J. Chandrasekhar, G. W. Spitznagel, P. v. R. Schleyer, *J. Comput. Chem.* **1983**, *4*, 294.
[33] A. D. McLean, G. S. Chandler, *J. Chem. Phys.* **1980**, *72*, 5639.
[34] M. J. Frisch, J. A. Pople, J. S. Binkley, *J. Chem. Phys.* **1984**, *80*, 3265.
[35] K. A. Peterson, S. S. Xantheas, D. A. Dixon, T. H. Dunning, *J. Phys. Chem. A* **1998**, ***102***, 2449.
[36] T. B. Tai, D. J. Grant, M. T. Nguyen, D. A. Dixon, *J. Phys. Chem. A* **2010**, *114*, 994.
[37] M. T. Nguyen, M. H. Matus, V. T. Ngan, D. J. Grant, D. A. Dixon, *J. Phys. Chem. A* **2009**, *113*, 4895.
[38] L. A. Curtiss, P. C. Redfern, K. Raghavachari, *J. Chem. Phys.* **2007**, *126*, 084108.
[39] R. J. Bartlett, M. Musial, *Rev. Mod. Phys.* **2007**, *79*, 291, and references therein.
[40] a) T. H. Dunning, *J. Chem. Phys.* **1989**, *90*, 1007; b) R. A. Kendall, T. H. Dunning, R. J. Harrison, *J. Chem. Phys.* **1992**, *96*, 6796.
[41] M. Rittby, R. J. Bartlett, *J. Phys. Chem.* **1988**, *92*, 3033.
[42] P. J. Knowles, C. Hampel, H. J. Werner, *J. Chem. Phys.* **1993**, *99*, 5219.
[43] M. J. O. Deegan, P. J. Knowles, *Chem. Phys. Lett.* **1994**, *227*, 321.
[44] K. A. Peterson, D. E. Woon, T. H. Dunning, *J. Chem. Phys.* **1994**, *100*, 7410.
[45] a) T. Helgaker, W. Klopper, H. Koch, J. Nagel, *J. Chem. Phys.* **1997**, *106*, 9639; b) A. Halkier, T. Helgaker, P. Jørgensen, W. Klopper, H. Koch, J. Olsen, A. K. Wilson, *Chem. Phys. Lett.* **1998**, *286*, 243.
[46] a) M. Douglas, N. M. Kroll, *Ann. Phys.* **1974**, *82*, 89–155; b) B. A. Hess, *Phys. Rev. A* **1985**, *32*, 756–763; c) B. A. Hess, *Phys. Rev. A* **1986**, *33*, 3742–3748.
[47] W. A. de Jong, R. J. Harrison, D. A. Dixon, *J. Chem. Phys.* **2001**, *114*, 48.
[48] EMSL basis set library. http://www.emsl.pnl.gov/forms/basisform.html.
[49] C. G. Zhan, F. Zheng, D. A. Dixon, *J. Am. Chem. Soc.* **2002**, *124*, 14795.
[50] C. E. Moore, *Atomic Energy Levels as Derived from the Analysis of Optical Spectra, Vol. 1, H to V*, U. S. National Bureau of Standards Circular 467,

U.S. Department of Commerce, National Technical Information Service, COM-72-50282, Washington, D. C., **1949**.
[51] A. Karton, J. M. L. Martin, *J. Phys. Chem. A* **2007**, *111*, 5936.
[52] L. A. Curtiss, K. Raghavachari, P. C. Redfern, J. A. Pople, *J. Chem. Phys.* **1997**, *106*, 1063.
[53] A. E. Reed, L. A. Curtiss, F. Weinhold, *Chem. Rev.* **1988**, *88*, 899.
[54] R. Wang, D. Zhang, R. Zhu, C. Liu, *J. Mol. Struct. THEOCHEM.* **2007**, *817*, 119.
[55] P. J. Garratt, *Aromatictity*, Wiley, New York, **1986**.
[56] D. Y. Zubarev, A. I. Boldyrev, *J. Comput. Chem.* **2006**, *28*, 251.
[57] a) T. Höltzl, N. Veldeman, J. De Haeck, T. Veszpremi, P. Lievens, M. T. Nguyen, *Chem. Eur. J.* **2009**, *15*, 3970; b) V. T. Ngan, P. Grune, P. Claes, E. Janssens, A. Fielicke, M. T. Nguyen, P. Lievens, *J. Am. Chem. Soc.* **2010**, *132*, 15589.

Received: May 5, 2011
Revised: August 14, 2011
Published online on October 7, 2011

